

UNSUPERVISED SEGMENTATION OF SMALLHOLDER FIELDS IN MOZAMBIQUE USING PLANETSCOPE IMAGERY

M. C. A. Picoli ^{1,2*}, J. Radoux ¹, X. Tong ², A. Bey ¹, P. Rufin ^{1,3}, M. Brandt ², R. Fensholt ², P. Meyfroidt ^{1,4}

¹ Earth and Life Institute, UCLouvain, 1348 Louvain-La-Neuve, Belgium - (michelle.picoli, patrick.meyfroidt, julien.radoux, adia.bey, philippe.rufin)@uclouvain.be

² Dept. of Geosciences and Natural Resource Management, University of Copenhagen, Copenhagen, Denmark - (xito, mabr, rf)@ign.ku.dk

³ Geography Department, Humboldt-Universität zu Berlin, Berlin, Germany

⁴ F.R.S.- FNRS, Brussels, Belgium - patrick.meyfroidt@uclouvain.be

KEY WORDS: Object-based image analysis (OBIA), smallholders, mean shift, multiresolution, SNIC.

ABSTRACT:

Smallholders produce about a third of the global crop production. Supporting these smallholder farms is an important lever for poverty alleviation. Farm and field sizes are key indicators of many smallholder dynamics, including fragmentation, farm consolidation, and interactions between smallholders, medium-scale commercial farming, and large enterprises. Despite the socio-economic, environmental, and political importance of these dynamics, spatially explicit data on farms and field sizes are still lacking. Identifying small-scale agriculture using satellite imagery is challenging due to the heterogeneity in the crop types and management practices. This study compared three unsupervised segmentation approaches that have not been widely explored for delineating smallholder fields: mean shift, multiresolution segmentation, and simple non-iterative clustering (SNIC), using PlanetScope imagery. The study area is located in northern Mozambique, where 71% of the farms cover less than 2 ha. The results were evaluated using four segmentation accuracy metrics based on object geometries: Area Fit Index (AFI), Quality Rate (QR), Oversegmentation (OS), and Undersegmentation (US). The results showed that the multiresolution segmentation algorithm outperformed the other methods to delineate smallholder fields. This work will support future regional-scale mapping efforts.

1. INTRODUCTION

Farm and field sizes are key indicators of many smallholder dynamics, including fragmentation, farm consolidation, and interactions between smallholders, medium-scale commercial farming, and large enterprises. Farms covering less than 2 ha of land occupy an estimated 24% of the gross agricultural area, producing 28-31% of the global crop production and 30-34% of the food supply, as extrapolated from the 55 countries studied by Ricciardi et al. (2018). Small farms have high crop diversity and productivity, regulate ecosystem processes, increase system resilience, and impact poverty reduction (Wiggins, 2009; van Vliet et al., 2015; Ricciardi et al., 2018; Julien et al., 2019; Ricciardi et al., 2021). These issues are crucial in Mozambique, where ~66% of the population resides in rural areas (INE, 2020), 71% of the agricultural holdings are <2 ha, and where agriculture is the main source of income for 80% of smallholders (CGAP, 2016).

Despite the socio-economic, environmental, and political importance of smallholder dynamics, spatially explicit data on small farms is still severely lacking. Identifying small-scale agriculture using satellite images is challenging due to high fragmentation and heterogeneity in land use, crop types, and management practices (Julien et al., 2019; Ruffin et al., 2022).

Unsupervised approaches are particularly valuable in contexts where abundant training data for supervised approaches is lacking, costly, and difficult to collect. In this study, we compared three unsupervised segmentation approaches that have not been widely explored for delineating smallholder fields, namely mean shift, multiresolution segmentation, and simple

non-iterative clustering (SNIC), using PlanetScope imagery with a spatial resolution of 3.7 m.

We evaluated the results using four supervised metrics, which use reference data to assess segmentation accuracy. This comparison will support future regional-scale mapping efforts, where there is still a lack of accurate information on field sizes.

2. BACKGROUND

2.1 Mean shift

The mean shift algorithm, proposed by Fukunaga and Hostetler (1975), is a non-parametric method that detects groups of samples by characteristic similarity, i.e., it detects groups of points in the feature space. This method was later adapted by Cheng (1995) for applications in Computer Vision, and more recently, this method was extended to be applied in image segmentation by Comaniciu and Meer (2002).

The principle of this algorithm is not to make assumptions about the shape of the distribution or the number of groups in an image. In this way, the groups in the n-dimensional attribute space can be modelled through an empirical probability density function, in which dense regions in this space correspond to the maximum or local modes of distribution (Derpanis, 2005).

The segmentation is created by the grouping of pixels that converge to a certain mode in the spatial domain and in the attribute space so that the pixel will receive the label of a group according to its proximity to this group, considering these two domains (Comaniciu and Meer, 2002; Derpanis, 2005). The

* Corresponding author

mean shift algorithm is implemented in the Orfeo Toolbox available in QGIS.

2.2 Multiresolution segmentation

The second algorithm, Multiresolution Segmentation, is a region-based algorithm that uses a bottom-up region merging technique (Baatz and Schäpe, 2000). It starts by considering each pixel as a separate object and then merges pairs of objects to form larger segments.

The optimization procedure minimizes the internal weighted heterogeneity of each object. The object is incremented until the smallest increment exceeds the threshold defined by the scale parameter, when this occurs, the process is stopped (Beenz et al., 2004). The scale parameter defines the heterogeneity of pixels, which indirectly determines the object's size.

The homogeneity criterion is defined by weighting two parameters of both segment and its border: color/shape (balances the homogeneity of the segment color with its shape) and compactness/smoothness (balances the smoothness of the segment border with its compactness). The algorithm is implemented in the eCognition Developer software for Object-Based Image Analysis (OBIA) applications.

2.3 Simple Non-linear Iterative Clustering (SNIC)

The Simple Non-linear Iterative Clustering (SNIC) algorithm (Achanta and Süsstrunk, 2017) is based on the Simple Linear Iterative Clustering (SLIC) (Achanta et al., 2012). This algorithm calculates the distance from each group center to pixels that are within a predefined search radius. According to Achanta et al. (2012), the distance between a group and an element combines normalized spatial and color distances.

SNIC creates a regular grid controlled by the approximate number of superpixels desired by the user. After that, each pixel overlapped by the search radius is associated with the center of the nearest cluster. SNIC can update cluster centers online in one iteration. Starting from the initial seed point, the SNIC algorithm uses a priority queue to select the next pixel to add to a superpixel. By normalizing the spatial distance between the centroid and the pixel by a constant (equivalent to the dimension of the centroid region) and determining a weight factor to define the degree of importance for the spatial distance concerning the distance in the color space, it is possible to control the compactness of the generated segments. So that the smaller the value of the weight factor, the more adherent the superpixels will be to the object's borders.

When the algorithm is executed, the priority queue is emptied to attribute labels at one end and filled with new candidates at the other end. The algorithm will terminate when there are no remaining unlabeled pixels to add new elements to the queue and empty the queue (Achanta and Süsstrunk, 2017). The Simple Non-Iterative Clustering algorithm is available in the Google Earth Engine platform.

3. MATERIAL AND METHOD

3.1 Study area

The study area covers ~35,100 ha in the Gurué district, within Zambézia province, Mozambique. This predominantly

smallholder region has experienced a surge in foreign agricultural investments through large-scale land acquisitions over the last decades (Bey et al., 2020), as well as the development of medium-scale farming (Baumert and Nhantumbo, 2017) and has an increasingly heterogeneous agriculture profile.

The main crops produced on a small scale are maize, cassava, beans, pigeon peas, millet, sorghum, peanuts, and now soybeans, and those on a large scale are macadamia nuts and tea (Joala et al., 2016).

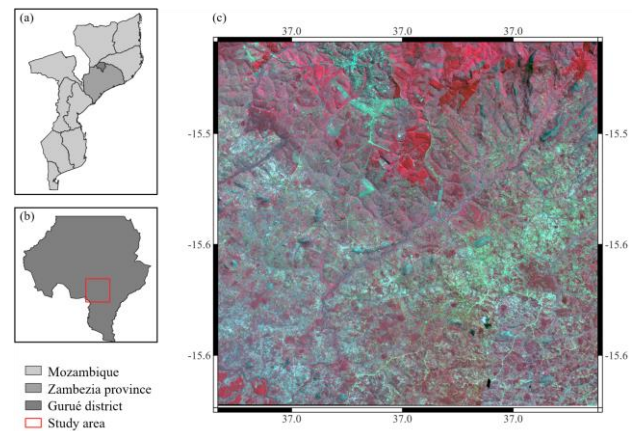


Figure 1. Study area. (a) Mozambique country-level map, (b) Gurué district-level map, (c) PlanetScope imagery of study area false-color composite (R: near-infrared, G: red, B: green).

3.2 Data

PlanetScope is a satellites constellation comprising approximately 130 CubeSats in a sun-synchronous orbit, operated by Planet Labs (Planet Labs, 2022). The used PlanetScope images contain four spectral bands: blue (455–515 nm), green (500–590 nm), red (590–670 nm), and near-infrared (NIR, 780–860 nm), with a spatial resolution of approximately 3 m.

This study used Level-3B surface reflectance images atmospherically corrected by Planet Labs, collected between April and May 2019 (Planet Labs PBC, 2018). The available images were combined into a cloud-free mosaic covering the study area.

3.3 Method

The first segmentation algorithm, mean shift, was applied over the four PlanetScope bands using Orfeo ToolBox (Grizonnet et al., 2017) in QGIS software. Different thresholds were tested for range radius (5 and 15) and minimum region size (20, 40, and 60).

To test the second algorithm, multiresolution segmentation, we first used the Estimation of Scale Parameters tool for multiband images (ESP2 tool, in eCognition software) to select the scale parameter (SP) (Dragut et al., 2014). In addition to the SP values calculated by the ESP2 tool, we tested another SP value (SP: 20¹, 46¹, and 75; shape: 0.8; compactness: 0.5). We ran the multiresolution segmentation on the four PlanetScope bands.

We applied the third and final algorithm, the simple non-iterative clustering (SNIC), on the Google Earth Engine platform, using the four PlanetScope bands, with size: 3, compactness: 0,

¹ SP value estimated using the ESP2 tool

connectivity: 8, neighborhood size: 256, and seed grid size: 12 and 14.

3.4 Validation

We evaluated the segmentation accuracy of all algorithms using 90 random reference polygon samples digitized using PlanetScope images and the very-high-resolution images available on the Google Earth platform. For that, we first generated 90 random points within the study area. We created a 5 ha buffer around these points and digitized at least one agricultural field inside the buffer. The reference polygon geometries were compared with the segmentation results using four goodness metrics: Area Fit Index (AFI), Quality Rate (QR), Oversegmentation (OS), and Undersegmentation (US) (Lucieer and Stein, 2002; Weidner, 2008; Clinton et al., 2010).

The AFI is a global metric used to identify both OS and US. AFI equal to 0 indicates a perfect segmentation, where the segments correspond exactly to the reference objects. Positive values of the AFI metric indicate that the methods result in oversegmentation compared to the reference polygons, while negative values indicate undersegmentation (Lucieer and Stein, 2002). The global QR metric varies between 0 and 1, where the optimal value is 0 (Weidner, 2008). The OS metric measures the oversegmentation error, which occurs when unnecessary boundaries are delimited, i.e., the objects resulting from the segmentation are smaller than the reference polygons (Clinton et al., 2010). The US metric measures the undersegmentation error, which occurs when the segmentation fails to define the boundaries of the objects, generating objects larger than the reference polygons (Clinton et al., 2010). A perfect match between a reference polygon and the segment object results in an OS and US equal 0.

These metrics are implemented in the *segmetric* R package (Simoes et al., 2022) and are presented in Table 1.

Metric	Range	Optimal value
$AFI = \frac{area(x_i) - area(y_j)}{area(x_i)}$	$(-\infty, \infty)$	0
$QR = 1 - \frac{area(x_i \cap y_j)}{area(x_i \cup y_j)}$	[0, 1]	0
$OS = 1 - \frac{area(x_i \cap y_j)}{area(x_i)}$	[0, 1]	0
$US = 1 - \frac{area(x_i \cap y_j)}{area(y_j)}$	[0, 1]	0

Table 1. Metrics used to evaluate the segmentation accuracy. x_i refers to reference polygons and y_i to the segmentation objects.

4. RESULTS

We applied three segmentation methods to delineate agricultural fields for a landscape rich in small-size farms in northern Mozambique. Figure 2 presents the segments generated by the three algorithms in a region with a high concentration of smallholder fields ($\sim < 0.3$ ha). We identified for each algorithm the best performing set of parameters according to the calculated metrics (Figure 2b, d, and g, Table 2).

The mean shift algorithm tends to segment the landscape into smaller objects (Figure 2a, b, and c), generating an oversegmentation reflected in high OS metrics.

In contrast, the multiresolution algorithm with SP values of 46 and 75 undersegmented the small crop fields (Figures 2e and f). With an SP value of 20, the multiresolution algorithm separates trees and small areas containing some vegetation from crop fields (Figure 2d).

Figure 3 presents the segmentations generated for an area with medium fields (~ 3.6 ha). This Figure shows that all three algorithms in the presented parametrization generally oversegmented the fields. However, with SP equal to 75, the multiresolution algorithm could delineate medium-sized fields boundaries more accurately (Figure 3f).

Based on the four goodness metrics (AFI, QR, OS, and US), the multiresolution method produced the best performing segmentation concerning small fields, which dominate this landscape (Table 2). The algorithm that most oversegmented the fields was mean shift using the parameters ranges radius equal to 5 and 15 and minimum region size equivalent to 20 and 40 (see AFI and OS metrics, Table 2), as shown in Figures 2 and 3.

The multiresolution algorithm using the ESP2 tool for SP estimation was more accurate in delineating the small agricultural fields (with SP=20) and medium fields (with SP=75).

We used reference polygons of small and medium fields to assess the quality of segmentation algorithms and calculate the metrics in Table 2, as there are no large agricultural fields in the study area. However, as observed in Figures 2 and 3, it is not possible to delineate both small and medium boundary fields simultaneously using only one parameter set. Therefore, it will be necessary for future studies to develop a method that combines different segmentation parametrizations to estimate the field size across a range from small to medium to large fields.

Method	AFI	QR	OS	US
(a) Mean shift	0.59	0.92	0.92	0.1
(b) Mean shift	-0.03	0.82	0.78	0.16
(c) Mean shift	0.31	0.87	0.85	0.13
(d) Multiresolution	0.15	0.76	0.74	0.18
(e) Multiresolution	-1.78	0.60	0.30	0.39
(f) Multiresolution	-9.29	0.79	0.17	0.72
(g) SNIC	-0.1	0.91	0.89	0.11
(h) SNIC	-0.41	0.89	0.86	0.13

Table 2. Segmentation assessment metrics: Area Fit Index (AFI), Quality Rate (QR), Oversegmentation (OS), and Undersegmentation (US). The best results are highlighted (with zero being the ideal value). (a) Mean shift: range radius = 5, minimum region size = 20; (b) Mean shift: range radius = 5, minimum region size = 60; (c) Mean shift: range radius = 15, minimum region size = 40; (d) Multiresolution: SP = 20, shape: 0.8, compactness: 0.5; (e) Multiresolution: SP = 46, shape: 0.8, compactness: 0.5; (f) Multiresolution: SP = 75, shape: 0.8, compactness: 0.5; (g) SNIC: with size = 3, compactness = 0, connectivity = 8, neighborhood size = 256, seed grid size = 12; (h) SNIC: with size = 3, compactness = 0, connectivity = 8, neighborhood size = 256, seed grid size = 14.

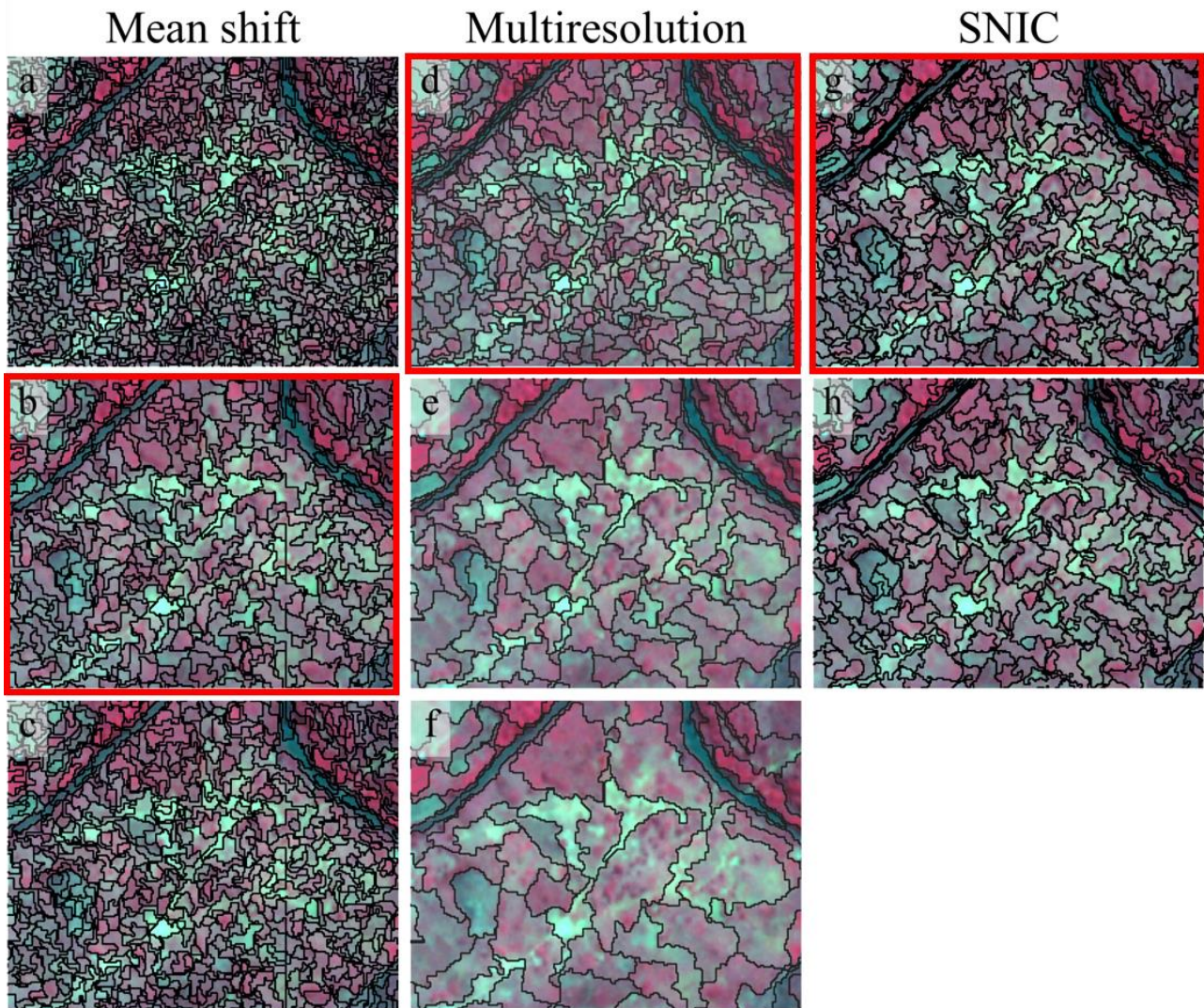


Figure 2. Segmentation results for smallholder farms. (a) Mean shift: range radius = 5, minimum region size = 20; (b) Mean shift: range radius = 5, minimum region size = 60; (c) Mean shift: range radius = 15, minimum region size = 40; (d) Multiresolution: SP = 20, shape: 0.8, compactness: 0.5; (e) Multiresolution: SP = 46, shape: 0.8, compactness: 0.5; (f) Multiresolution: SP = 75, shape: 0.8, compactness: 0.5; (g) SNIC: with size = 3, compactness = 0, connectivity = 8, neighborhood size = 256, seed grid size = 12; (h) SNIC: with size = 3, compactness = 0, connectivity = 8, neighborhood size = 256, seed grid size = 14. The best performing set of parameters for each algorithm is highlighted by a red square (b: mean shift, d: multiresolution, g: SNIC).

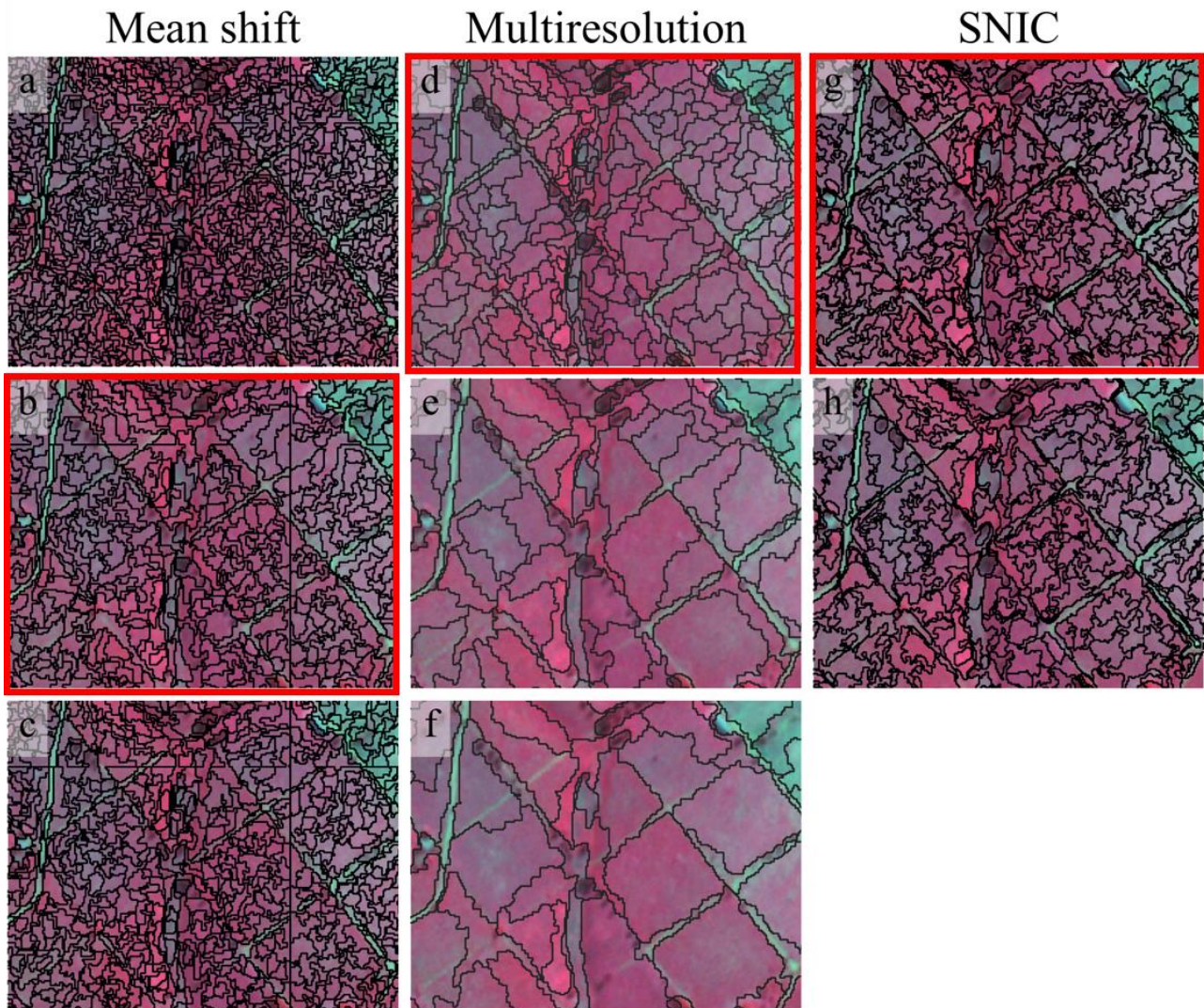


Figure 3. Segmentation results for medium farms. (a) Mean shift: range radius = 5, minimum region size = 20; (b) Mean shift: range radius = 5, minimum region size = 60; (c) Mean shift: range radius = 15, minimum region size = 40; (d) Multiresolution: SP = 20, shape: 0.8, compactness: 0.5; (e) Multiresolution: SP = 46, shape: 0.8, compactness: 0.5; (f) Multiresolution: SP = 75, shape: 0.8, compactness: 0.5; (g) SNIC: with size = 3, compactness = 0, connectivity = 8, neighborhood size = 256, seed grid size = 12; (h) SNIC: with size = 3, compactness = 0, connectivity = 8, neighborhood size = 256, seed grid size = 14. The best performing set of parameters for each algorithm is highlighted by a red square (b: mean shift, d: multiresolution, g: SNIC).

5. CONCLUSION

Segmentation of very high-resolution remote sensing imagery is an important step for estimating the field size in a smallholder system. In this study, we compared the performance of three widely used segmentation algorithms: mean shift, multiresolution segmentation, and SNIC, using PlanetScope images at a spatial resolution of 3.7 meters. We determined the segmentation parameters based on several tests and an unsupervised estimation tool (ESP2).

We evaluated the accuracy of the segmentations using four goodness metrics commonly used in the literature. We observed that most of the combinations of parameters and algorithms tested here oversegmented the fields.

Among the three methods evaluated, Multiresolution combined with ESP2 for SP selection proved satisfactory and could be applied on a regional scale due to its accuracy and operability. However, we observed that it is not possible to simultaneously delineate small and medium fields boundaries using only one parameter in the studied region. Thus, it is necessary to develop a method that merges the segmentations of small and medium fields according to spectral criteria and field shape.

Nevertheless, by adopting a step-wise approach to identify small and medium sized fields sequentially, this study demonstrates that unsupervised algorithms – in conjunction with high spatial resolution PlanetScope imagery – can effectively delineate smallholder fields in contexts where reference data are scarce.

ACKNOWLEDGEMENTS

This research was supported by the European Research Council (ERC) under the European Union's Horizon 2020 research and innovation program (Grant agreement No 677140 MIDLAND) and the FRS-FNRS (grant no. T.0154.21).

REFERENCES

Achanta, R., Süsstrunk, S., 2017. Superpixels and polygons using simple non-iterative clustering. *Proceedings of the 30th IEEE Conference on Computer Vision and Pattern Recognition, CVPR 2017*, Honolulu, HI, USA, 21–26 July 2017.

Baatz, M., Schape, A., 2000. Multiresolution Segmentation: An Optimization Approach for High Quality Multi-Scale Image Segmentation. Strobl, J., Blaschke, T. and Griesbner, G. (Eds.), *Angewandte Geographische Informations-Verarbeitung*, Wichmann Verlag, Karlsruhe, Germany, 12-23.

Baumert, S., Nhantumbo, I., 2017. Small-scale soya farming can outperform large-scale agricultural investments. International Institute for Environment and Development.

Bey, A., Jetimane, J., Lisboa, S.N., Ribeiro, N., Siteo, A., Meyfroidt, P., 2020. Mapping smallholder and large-scale cropland dynamics with a flexible classification system and pixel-based composites in an emerging frontier of Mozambique. *Remote Sens. of Environment*, 239, 111611.

CGAP – Consultative Group to Assist the Poor, 2016. National Survey and Segmentation of Smallholder Households in Mozambique. The Consultative Group to Assist the Poor.

Cheng, Y., 1995. Mean shift, mode seeking, and clustering. *IEEE Trans. Pattern Anal. Mach. Intell.* 17, 790-799.

Clinton, N., Holt, A., Scarborough, J., Yan, L., Gong, P., 2010. Accuracy assessment measures for object-based image segmentation goodness. *Photogramm. Eng. Remote. Sens.* 76, 289-299.

Comaniciu, D., Meer, P., 2002. Mean shift: A robust approach toward feature spaceanalysis. *IEEE Trans. Pattern Anal. Mach. Intell.* 24, 603–619.

Derpanis, K. G., 2005. Mean shift clustering. Lecture Notes. http://www.cse.yorku.ca/~kosta/CompVis_Notes/mean_shift.pdf (20 July 2021).

Drăguț, L., Csillik, O., Eisank, C., Tiede, D., 2014. Automated parameterisation for multi-scale image segmentation on multiple layers. *ISPRS Journal of photogrammetry and Remote Sensing*, 88, 119-127.

Fukunaga, K., Hostetler, L., 1975. The estimation of the gradient of a density function, with applications in pattern recognition. *IEEE Trans. on Inf. Theory.*, 21, 32-40.

Grizonnet, M., Michel, J., Poughon, V., Inglada, J., Savinaud, M. and Cresson, R., 2017. Orfeo ToolBox: open source processing of remote sensing images. *Open Geospatial Data, Software and Standards*, 2(1), 1-8.

INE – Instituto Nacional de Estatística, 2020. Statistical Yearbook 2020 – Mozambique.

Joala, R., Zamchiya, P., Ntauazi, C., Musole, P. and Katebe, C., 2016. Changing agro-food systems: The impact of big agro-investors on food rights. Case studies in Mozambique and Zambia. http://repository.uwc.ac.za/xmlui/bitstream/handle/10566/4570/joala_changing_agrofood_systems_2016.pdf?sequence=1&isAllowed=y (2 August 2021).

Julien, J. C., Bravo-Ureta, B. E., Rada, N. E., 2019. Assessing farm performance by size in Malawi, Tanzania, and Uganda. *Food Policy*, 84, 153-164.

Lucieer, A., Stein, A., 2002. Existential uncertainty of spatial objects segmented from satellite sensor imagery. *Geosci. Remote. Sens. IEEE Trans.* 40, 2518-2521.

Planet Labs, 2022. PlanetScope. <https://developers.planet.com/docs/data/planetscope/> (5 March 2022).

Planet Labs PBC, 2018. Planet Application Program Interface: In Space for Life on Earth. San Francisco, CA. <https://api.planet.com>. (10 June 2021).

Ricciardi, V., Ramankutty, N., Mehrabi, Z., Jarvis, L., Chookolingo, B., 2018. How much of the world's food do smallholders produce?. *Global food security*, 17, 64-72.

Ricciardi, V., Mehrabi, Z., Wittman, H., James, D., Ramankutty, N., 2021. Higher yields and more biodiversity on smaller farms. *Nature Sustainability*, 4, 651-657.

Rufin, P., Bey, A., Picoli, M., Meyfroidt, P., 2022. An operational framework for large-area mapping of active cropland and short-term fallows in smallholder landscapes using PlanetScope data. <https://doi.org/10.31223/X5P62F>

Simoes, R., Sanchez, A., Picoli, M. C. A., 2022. segmetric: Metrics for Assessing Segmentation Accuracy for Geospatial Data. R package version 0.1.0. <https://cran.r-project.org/web/packages/segmetric/index.html>

van Vliet, J. A., Schut, A. G., Reidsma, P., Descheemaeker, K., Slingerland, M., van de Ven, G. W., Giller, K. E., 2015. Demystifying family farming: Features, diversity and trends across the globe. *Global food security*, 5, 11-18.

Weidner, U., 2008. Contribution to the assessment of segmentation quality for remote sensing applications. *International Archives of Photogrammetry, Remote Sensing and Spatial Information Sciences*, 37(B7), 479-484.

Wiggins, S., 2009. Can the smallholder model deliver poverty reduction and food security, FAC Working Paper 08, Brighton: Future Agricultures Consortium.